American Journal of Environmental Sciences

Original Research Paper

Transverse Velocity, Transverse Boundary Shear Stress and Flow Deviation in Meandering Open Channels

Youssef Ismail Hafez

Independent Researcher, Egypt

Article history
Received: 15-05-2024
Revised: 21-06-2024
Accepted: 24-06-2024

Email: youssefhafez995@gmail.com

Abstract: This study presents a novel approach for characterizing the mechanics of flow in mildly meandering open channels, specifically focusing on the development of a new vertical distribution equation for transverse velocity. Unlike existing equations in the literature that rely on complex logarithmic or integral forms or infinite series forms, which are impractical for hydraulic engineers, the proposed equation employs ordinary power functions. This new formulation offers several advantages, including the consideration of previously neglected lateral forces resulting from wind and ship movement. Comparisons with available existing equations indicate a good agreement, highlighting the accuracy, sensitivity to roughness, and applicability of the developed transverse velocity equation. Notably, the analysis reveals that wind velocities can significantly increase transverse surface and bed velocities, emphasizing the importance of considering such factors in flow characterization. Moreover, the present approach yields higher transverse surface and bed velocities compared to a well-known existing equation. The equation for transverse velocity relies on two key assumptions. Firstly, it assumes a constant turbulent viscosity throughout the flow. Secondly, it relies on the condition that the topographic steering number is less than one, allowing for the approximation of mild curvature and meandering conditions. In addition, the developed transverse velocity equation is the only equation that offers derivation for an expression for the transverse boundary shear stress. This expression accounts for the effects of the centripetal force and the transverse pressure force, providing a comprehensive understanding of the flow dynamics in meandering channels. The study further presents distinct expressions for the deviation angles of the flow velocity and the bed shear stress, enhancing our understanding of the complex mechanisms governing flow behavior in meandering channels.

Keywords: Meandering Open Channels, Transverse Velocity Vertical Distribution, Radial Boundary Shear Stress, Deviation Angle of the Flow Velocity, Deviation Angle of the Boundary Shear Stress

Introduction

Meandering channels, characterized by their twisting, curving, bending, and meandering sections, are ubiquitous in rivers and alluvial open channels worldwide. These meandering patterns extend over a significant portion of the channel length, highlighting the need for in-depth investigations into meanders. It is rare to find straight alluvial channels longer than approximately 10-12 channel widths, emphasizing the prevalence and significance of meandering phenomena (Odgaard, 1986a). Meandering channels are dynamic landforms that emerge as a result of fluid mechanics and sedimentary processes (Weiss and Higdon, 2022). Hafez (2022) attributes river meandering to the imbalance between the valley slope and the regime channel slope, considering it the primary cause when sediment load is less than the load transport capacity and bank erodibility permits.

Meandering is not limited to fluid systems such as natural rivers, channels, the Gulf Stream, and free-falling streams of viscous fluids. It is also observed in non-fluid systems, including derailed trains and jack-knifed trucks (Sahagian *et al*., 2022). The water flow discharge and sediment load play crucial roles in shaping and influencing river meander plan-forms (Hafez, 2022). Therefore, understanding the mechanics of flow and its

DOI: 10.3844/ajessp.2024.1.21

influence on sediment transport, channel morphology, and plan form is essential for comprehending the meandering phenomenon. The present study focuses on the mechanics of flow in curved meandering alluvial river channels, while the mechanics of sediment transport are addressed in a separate study.

Despite numerous studies on the flow mechanics of river meandering and advancements in computer power for two- and three-dimensional computations, as well as measurement techniques, several fundamental issues regarding flow mechanics and sediment transport in meandering channels remain unresolved, even within the context of one-dimensional analysis. Ferreira da Silva and Ebrahimi (2017) highlighted significant discrepancies between computer model results and reality, emphasizing the need for a deeper understanding of the underlying physical processes and improved analytical descriptions.

Early analytical works yielded equations for the transverse velocity distribution in meandering channels, such as those proposed by Rozovskii (1961); Kikkawa *et al*. (1976); Ascanio and Kennedy (1983). However, these equations often involve complex functions, such as integrals, logarithms, or infinite series, or rely on graphical functions, making them less attractive and less user-friendly. Furthermore, important factors such as wind effects on the transverse velocity vertical profile and the transverse boundary shear stress have not been adequately addressed in these equations. While investigations exist on wind effects, they have primarily focused on river plume dynamics rather than meandering channels (Elbagoury *et al*., 2023).

Although pioneering works by Rozoviskii (1961); Engelund (1974); Kikkawa *et al*. (1976); Bridge (1977); Odgaard (1981; 1982; 1984; 1986a-b); Ascanio and Kennedy (1983); Chang (1983; 1984; 1988) significantly contributed to the understanding of flow mechanics in curved open channels and rivers, limited analysis has been conducted in a similar vein since then. Most of these investigations focused on one-dimensional open channel flow. In recent decades, researchers have turned to two- and three-dimensional numerical investigations (Gu *et al*., 2016; Krzyk and Cetina, 2018; Pradhan *et al*., 2018; Bai *et al*., 2019; Thappeta *et al*., 2020; Zhou and Endreny, 2020). However, these studies often lack a comprehensive analytical framework and fail to provide equations that govern and explain the flow mechanics process. While valuable for understanding the influence of curvature on the velocity field, they are insufficient for thorough analysis. An exception is the two-dimensional water surface model by Molinas and Hafez (2000), which numerically investigates the effects of roughness, depth, and energy slope on the curving flow field around vertical wall abutments and develops an analytical expression for nose velocity amplification versus the friction factor.

Despite the advancements in two- and three-dimensional numerical models for curved flow fields, certain issues remain unresolved even within the one-dimensional context, necessitating further developments. Similar situations exist, for example as by Nowroozpour *et al*. (2022) who suggest flow in alluvial, open-channel contractions requires further investigation as they observed that trends in the depth of contraction scour, especially live-bed scour, to deviate from the trends suggested by common guidelines.

In the context of one-dimensional investigations of transverse velocity in meandering channels, past works mostly consist of complex equations that are difficult to apply and adapt in numerical and analytical studies. Moreover, some assumptions made in previous studies can be improved upon. Most two-dimensional flow models adopt depth-averaged equations (e.g., He, 2018; Park and Ahn, 2019), which neglect vertical variations in velocity profiles and boundary shear stress. While these models are valuable for understanding the overall flow patterns, they do not provide detailed information on the flow mechanics within the channel cross-section. The depth-averaging process yields by definition net zero lateral velocity component along the fully developed flow region as can be seen in the graphical flow fields that the resultant velocity vector turns or curves more or less in the same manner as the turning or curving of the channel axis and walls. Molinas and Hafez (2000) avoided this situation by developing a 2D model along the water surface in which the lateral velocity component exists in the fully developed zone and at its maximum value contrary to being near zero in depth-averaged models.

In the meantime, recent experimental investigations such as Pradhan *et al*. (2018); Bai *et al*. (2019) are focusing mostly on measurements of velocity. However, lack of in-depth analysis has not guided these experimental investigations to produce useful empirical equations or useful measuring of the quantities that are really required in analytical and numerical studies such as transverse energy loss slope, transverse boundary shear stress, roughness in curved channels, transverse sediment transport …etc. In the experiments of He *et al*. (2021) two laboratorial sine-generated channels, i.e., one with deflection angle = 30° and the other at 110° no flow velocities and also no transverse bed slopes were reported. Intensive field data collection of the geometric parameters of 1499 bends, Zhou and Tang (2022), using Landsat images in the Yimin River China, yet no hydraulic and sediment data were collected in order to relate them to the meander patterns. This addresses the lack of incomplete data sets necessary for development, testing, and validation.

In this study, some of the fundamental assumptions in the pioneering works are revisited and modified in addition to presenting equations in an attractable and user-friendly form which allows their inclusion in analytical and numerical models. For example, a novel equation for the

DOI: 10.3844/ajessp.2024.1.21

vertical distribution of the transverse velocity in a curved open channel is developed. This equation, which uses typical or ordinary power functions, has the advantage of being attractive, easy to apply, inclusive of transverse wind and ship forces, easy to derive from it an expression for the lateral boundary shear stress, and easy for inclusion in analytical and numerical models. In addition, expression is developed for boundary shear stress deviation angle which differentiates it from the flow velocity deviation angle. The equation for transverse velocity relies on two key assumptions. Firstly, it assumes a constant turbulent viscosity throughout the flow. Secondly, it relies on the condition that the topographic steering number is less than one, allowing for the approximation of mild curvature and meandering conditions.

To address the limitations and gaps in the current understanding of flow mechanics in meandering channels, this research tries to develop improved analytical frameworks useful for meandering analytical investigations and numerical models. These advancements should consider factors such as wind effects, applicable vertical variations in transverse velocity profiles, and reliable transverse boundary shear stress.

In conclusion, meandering channels are complex systems influenced by fluid mechanics and sedimentary processes. While significant progress has been made in understanding flow mechanics in meandering channels, several fundamental issues remain unresolved as stated before. Further research is needed to develop improved analytical frameworks and numerical models that consider various factors and provide a comprehensive understanding of flow mechanics in meandering channels. This need motivated the present study in trying to improve the existing knowledge regarding transverse velocity vertical distribution, transverse boundary shear stress, and flow and boundary shear deviation angles.

Review of Curved Channel Flow Mechanics

The starting point for the analytical and numerical investigations of meandering channels is the equations of fluid motion in curved open channels. It is assumed here that the flows are subcritical and the pressure is hydrostatic, which is often the case under most field conditions. Under these conditions the equations of motion in the longitudinal and radial (transverse or lateral) directions are expressed, Chang (1988) and Fig. (1), as:

$$\frac{\partial u}{\partial t} + u\frac{\partial u}{\partial s} + v\frac{\partial u}{\partial r} + w\frac{\partial u}{\partial z} = -\frac{u v}{r} + g S + \frac{1}{\rho}\frac{\partial \tau_s}{\partial z} \quad (1)$$

$$\frac{\partial v}{\partial t} + u\frac{\partial v}{\partial s} + v\frac{\partial v}{\partial r} + w\frac{\partial v}{\partial z} = \frac{u^2}{r} - g S_r + \frac{1}{\rho}\frac{\partial \tau_r}{\partial z} \quad (2)$$

where, as in Fig. (1) u is the primary (longitudinal or main) flow local velocity, t is the time, s is the curvilinear coordinate along the channel main direction, v is the lateral (radial or transverse) local velocity, r is the radial direction measured from the center of curvature of the bend, w is the vertical local velocity, z is the vertical coordinate measured from the bed level upward, g is the acceleration due to gravity, S is the channel longitudinal slope, ρ is the fluid density, τ_s is the longitudinal local turbulent shear stress, S_r is the transverse water surface slope and τ_r is the radial or transverse local turbulent-shear stress. In Eq. (2) the term (u^2/r) represents the centripetal force (per unit mass) while the term ($g\ S_r$) represents the radial pressure force (per unit mass) which is associated with the transverse water surface slope or inclination (S_r) due to the assumption of the hydrostatic pressure distribution.

Assuming wide channels (in the central region) some assumptions could be made. It could be assumed in the central region that the vertical velocity w is small (w is of second order) and uniformity of all the variables could be assumed, i.e., derivatives with respect to r can be neglected. Assuming further mild curvature or a large relatively channel radius, r, the quantity ($u\ v/r$) could be assumed small and therefore neglected. In addition, steady flows (time derivatives are zeros) and fully developed conditions are assumed (uniform flow where all derivatives with respect to s are assumed zeros). Under these conditions, Eqs. (1-2) reduce to:

$$g S + \frac{1}{\rho}\frac{\partial \tau_s}{\partial z} = 0 \quad (3)$$

$$\frac{u^2}{r} - g S_r + \frac{1}{\rho}\frac{\partial \tau_r}{\partial z} = 0 \quad (4)$$

Equation (3) gives a linear distribution of the longitudinal shear stress as:

$$\tau_s = \rho\, g\, (D - z)\, S \quad (5)$$

where, D is the local flow depth. By assuming isotropic turbulence, Chang (1988), the turbulent shear stresses τ_s and τ_r can be expressed in terms of the isotropic eddy viscosity and the respective velocity gradient, that is:

$$\frac{\tau_s}{\rho} = \nu_T \frac{\partial u}{\partial z} \quad (6)$$

and:

$$\frac{\tau_r}{\rho} = \nu_T \frac{\partial v}{\partial z} \quad (7)$$

where, ν_T is the isotropic turbulent eddy viscosity.

Among the first investigations of the lateral or transverse (radial) velocity, distribution is that by Rozovskii (1961). He assumed the following logarithmic longitudinal velocity distribution:

$$\frac{u}{\overline{U}} = 1 + \frac{g^{1/2}}{\kappa C}(1 + \ln \eta) \quad (8)$$

where, $\overline{U}$ is the depth-averaged longitudinal velocity, κ is the von Karman constant ($\kappa = 0.4$ in clear fluid), C is the Chezy's roughness coefficient, $\eta = z/D$ is the relative depth and D is the local flow depth.

DOI: 10.3844/ajessp.2024.1.21

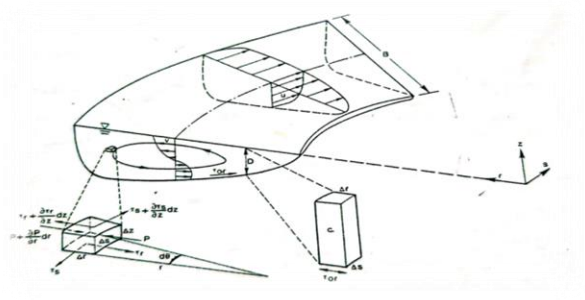

Fig. 1: Definition sketch for flow in a curved open channel, after Chang (1988)

Rozovskii (1961) used Eq. (8) to derive the following formula for the transverse velocity in the case of smooth channel bottom:

$$\frac{v}{\bar{U}} = \frac{1}{\kappa^2}\frac{D}{r}\left[F_1(\eta) - \frac{g^{1/2}}{\kappa C}F_2(\eta)\right] \quad (9)$$

where, $F_1(\eta)$ and $F_2(\eta)$ are functions of the relative depth which are given as:

$$F_1(\eta) = \int \frac{2\ln\eta}{\eta-1}\,d\eta \quad (10)$$

$$F_2(\eta) = \int \frac{\ln^2\eta}{\eta-1}\,d\eta \quad (11)$$

In the case of the rough channel bottom, Rozovskii (1961) presented the following formula:

$$\frac{v}{\bar{U}} = \frac{1}{\kappa^2}\frac{D}{r}\left[F_1(\eta) - \frac{g^{1/2}}{\kappa C}\{F_2(\eta) + 0.8\,(1 + ln\,\eta)\}\right] \quad (12)$$

The two functions $F_1(\eta)$ and $F_2(\eta)$ in Eqs. (10-11) which are evaluated through integration formulas and are also given in graphical forms, however, it is not practical for the hydraulic engineers to use them. This constitutes difficulty when the profile of the radial velocity is required in analytical investigations as was required in Chang (1983); Hafez (2023) for the evaluation of the transverse energy loss slope. Such difficulty also arises when requiring the vertical profile for the radial velocity in numerical models such as meander path models, Chang (1984); Odgaard (1986a) as input to the meander path model. In both Eq. (8) for the longitudinal velocity *u* and Eq. (12) for the transverse velocity *v*, the presence of *ln* (η) presents difficulty in evaluating the two velocity components and their derivatives at the bed (η = 0) as *ln* (η) and (1/η) are undefined at the bed where η = 0. The derivative of Eq. (9 or 12) is necessary to evaluate the transverse boundary shear stress; therefore it is not possible to use Rozovskii (1961) velocity profiles to evaluate the lateral bed shear stress.

On the other hand, Kikkawa *et al*. (1976), using the stream function approach in the equations of motion, presented the vertical distribution for the transverse velocity as:

$$v = F^2(r)\,\frac{U}{\kappa}\frac{D}{r}\left[F_A(\eta) - \frac{1}{\kappa}\frac{U_*}{U}F_B(\eta)\right] \quad (13)$$

where, $F(r)$ is the radial distribution of the depth-averaged main velocity ($\bar{U}$) normalized by U, U is the cross-sectional averaged velocity and U_* is the shear velocity of the cross-section. The two functions $F_A(\eta)$ and $F_B(\eta)$ are expressed in the form of logarithmic functions:

$$F_A(\eta) = -15\left[(\eta)^2\ln(\eta) - \frac{1}{2}(\eta)^2 + \frac{15}{54}\right] \quad (14)$$

and:

$$F_B(\eta) = \frac{15}{2}\left[(\eta)^2\ln^2(\eta) - (\eta)^2\ln(\eta) + \frac{1}{2}(\eta)^2 - \frac{19}{54}\right] \quad (15)$$

Hafez (2023) adopted Kikkawa *et al*. (1976) transverse velocity profile as given in Eq. (13) for evaluating the transverse energy-loss slope. However, the derivation is very lengthy due to the complex structure of Eqs. (14-15). This is due primarily that not only the seven terms appearing in the transverse velocity expression of Eq. (13) are required for manipulation in the derivation by Hafez (2023) but also evaluation of their derivatives is required which is not an easy task. It is noted in Rozovskii (1961) Eq. 12 and Kikkawa *et al.* (1976), Eq. (13), that due to the presence of the logarithmic function *ln* (η), the lateral bed shear stress could not be evaluated from these velocity distributions as the logarithmic function is undefined at η = 0. This is a major shortcoming of these two widely known equations for the lateral velocity in meandering channels.

Ascanio and Kennedy (1983) calculated the radial velocity assuming a linearly primary-flow shear stress, the power law for the main velocity, and an isotropic eddy viscosity. The power law is given as by Zimmerman and Kennedy (1978) as:

$$\frac{u}{\bar{U}} = \frac{m+1}{m}\,\eta^{1/m} = (1+p)\left(\frac{z}{D}\right)^p \quad (16)$$

where, m = (1/p) is an exponent in the primary-flow velocity power law and m is related to the Darccy Weibach friction factor and von Karman constant by:

$$m = \frac{1}{p} = \frac{1}{\kappa}\sqrt{\frac{f}{8}} \quad (17)$$

The power law was used in many meandering investigations such as Ascanio and Kennedy (1983); Chang (1983; 1984); Odgaard (1986a). Recently in a

DOI: 10.3844/ajessp.2024.1.21

different, although some similarity exists, Dey *et al*. (2023) adopted the power law for the stream-wise velocity in their investigation of flow over a downstream-skewed wavy bed in which flow curvature is in the vertical plane.

Ascanio and Kennedy (1983) presented the following distribution for the transverse velocity:

$$\frac{v}{\bar{U}} = 8\,\frac{D}{r}\sum_{j=0}^{\infty}\left\{\begin{array}{l}\dfrac{(m+1)^4}{m^2(m+2)}\left[\dfrac{1}{(3/m+2+j)(3/m+1+j)}-\dfrac{1}{(1/m+1+j)(1/m+j)}\right]\\ \eta^{1/m}-\dfrac{(m+1)^3}{m(m+2)}\left[\dfrac{\eta^{3/m+1+j}}{3/m+1+j}-\dfrac{\eta^{(1/m+j}}{(1/m+j}\right]\end{array}\right\} \quad (18)$$

Clearly, the infinite series form in Eq. (18) and its complicated structure precludes its use in analytical and numerical investigations of curved open channels and derivation from it as an expression for transverse boundary shear stress. It is not clear how many terms are required for convergence of the infinite series in Eq. (18).

Some linearized versions of the radial velocity have been used to facilitate its use in several meandering investigations. For example, in evaluating energy expenditure in curved open channels Chang (1983; 1988) used a linearized form of the radial velocity profile based on Kikkawa *et al*. (1976), Eq. (13), in the form:

$$v = \frac{2}{\kappa}\left(3.75-\frac{1.875}{\kappa}\frac{U_*}{U}\right)\left(z-\frac{D}{2}\right)\frac{U}{r_c} \quad (19)$$

where, r_c is the radius of curvature of the channel centre line.

Chang (1984) in his regular meander path model used a surface radial velocity, v_s, from Kikkawa *et al*. (1976) equation by setting $\eta = z/D = 1$ in Eq. (13) and obtained:

$$v_s = \frac{U}{\kappa}\frac{D}{r_c}\left[\frac{10}{3}-\frac{1}{\kappa}\frac{5}{9}\sqrt{\frac{f}{2}}\right] \quad (20)$$

where, f is the Darcy-Weisbach friction factor which has the advantage over the Chezy and Manning roughness coefficients because it is dimensionless. The lateral bed velocity (v_b) could also be obtained from Kikkawa *et al*. (1976) equation by setting $\eta = z/D = 0$ and observing that the product $\eta \ln(\eta)$ is zero at $\eta = 0$, to obtain:

$$v_b = \frac{15}{54}\frac{U}{\kappa}\frac{D}{r_c}\left[-15+\frac{19}{4\kappa}\sqrt{\frac{f}{2}}\right] \quad (21)$$

Odgaard (1986a) in his meander flow model also assumed a linear vertical profile for the transverse velocity given as:

$$v = 2\,v_s\left(\frac{z}{D}-\frac{1}{2}\right) = 2\,\frac{U}{\kappa}\frac{D}{r_c}\left[\frac{10}{3}-\frac{1}{\kappa}\frac{5}{9}\sqrt{\frac{f}{2}}\right]\left(\frac{z}{D}-\frac{1}{2}\right) \quad (22)$$

where, v_s is the value of v at the water surface obtained from Eq. (20). Odgaard (1986a) concluded that Eq. (22) (Eq. (4) in Odgaard (1986a)) is in good agreement with the data profiles by Rozovskii (1961); Kikkawa *et al*. (1976); Odgaard (1982), as in Fig. (2).

Due to the presence of the transverse velocity component, the resultant velocity vector assumes an angle of deviation, δ_v, with the channel tangential direction. From Eqs. (8-9) by Rozovskii (1961), this angle at any depth could be given in the case of smooth bottoms as:

$$\tan\delta_v(\eta) = \frac{v}{u} = \frac{1}{\kappa^2}\frac{D}{r}\frac{F_1(\eta)-\frac{g^{1/2}}{\kappa C}F_2(\eta)}{1+\frac{g^{1/2}}{\kappa C}(1+ln\,\eta)} \quad (23)$$

For two values of the Chezy coefficient (C = 60 and 30), Rozovskii (1961) found that channel roughness has a minor effect on the deviation angle near the bed (δ_{vb}) and obtained the following relation:

$$\tan\delta_{vb} \approx 11\,\frac{D}{r} \quad (24)$$

Equation (24) has been proved satisfactory with the laboratory and field data by Kondrat′ev (1959). However, Engelund (1974) obtained $\tan(\delta_{vb}) = 7\,D/r$ which may be due to the channel beds being rougher than those in Eq. (24). The dependency of flow deviation angle on channel roughness will be seen later in the results section using the present approach which casts some doubt on Eq. (24). Due to the existence of the *ln* (η) in Eq. (23) it is not possible to substitute $\eta = 0$ in order to obtain direct value for the flow deviation angle at the channel bed. This problem will be overcome in the present approach.

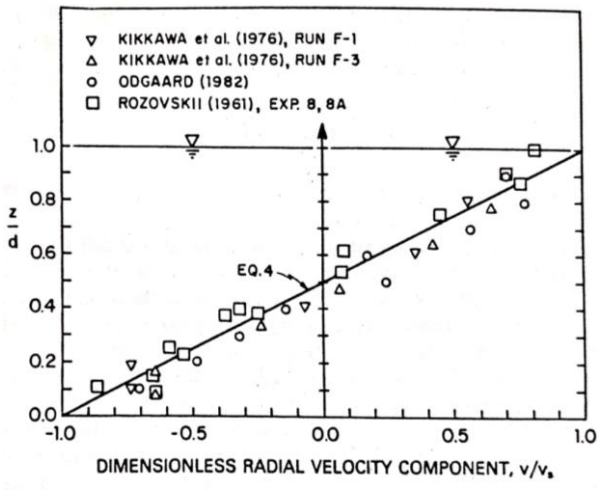

Fig. 2: Experimental vertical profiles of the transverse velocity and the linear approximation by Odgaard (1986b), Eq. (4) in the figure is Eq. (22) herein, after Odgaard (1986a)

DOI: 10.3844/ajessp.2024.1.21

Neglecting the transverse force contributed by the bed due to friction and boundary shear stress, Rozoveskii (1957); Yen (1965) balanced the pressure force by the centripetal force and obtained an equation for the transverse water surface slope as:

$$S_r = \frac{C_r\,\bar{U}^2}{g\,r} \tag{25}$$

where, C_r is a correction factor that accounts for the nonlinear distribution of the u velocity and $\bar{U}$ is the depth-averaged velocity used to replace the local velocity u. For a wide channel by assuming C_r =1, $\bar{U} = U$ and $r_c = r$, Chang (1988) simplifies Eq. (25) to:

$$S_r = \frac{U^2}{g\,r_c} \tag{26}$$

where, U is the cross-sectionally averaged velocity. Equation (26) has been widely used such as by Rozovskii (1961); Yen (1965); Chang (1984); Odgaard (1986a) among others.

Jansen *et al*. (1979) by using a radial velocity profile similar to Rozovskii (1961), Eq. (12), obtained the following equation for the radial component of the boundary shear stress (τ_{or}):

$$\tau_{or} = -\rho\,D\,\frac{U^2}{r}\left[2\left(\frac{g^{1/2}}{\kappa\,C}\right)^2 - 2\left(\frac{g^{1/2}}{\kappa\,C}\right)^3\right] \tag{27}$$

The negative sign indicates that the direction of the bed shear stress is inward toward the center of curvature. The tangential boundary stress is given by:

$$\tau_{os} = \rho\,g\,\frac{U^2}{C^2} \tag{28}$$

Equations (27-28) are used to calculate the angle between the resultant bed shear stress and the channel axis ($\delta_{\tau b}$) by Jansen *et al*. (1979) as:

$$\tan\delta_{\tau b} = \frac{\tau_{or}}{\tau_{os}} = -\frac{2}{\kappa^2}\frac{D}{r}\left(1 - \frac{g^{1/2}}{\kappa\,C}\right) \tag{29}$$

Ascanio and Kennedy (1983) balanced the moment due to the centrifugal acceleration by that due to the radial bed shear stress and obtained the relation:

$$\tau_{or} = \rho\,D\,\frac{U^2}{r}\,\frac{1+m}{(2+m)m} \tag{30}$$

where, "m" is given from Eq. (17). It is noted that Eq. (30) neglects the contribution by the transverse pressure force (transverse water surface slope, S_r) in spite that it is a key influencing factor in curved flows.

The foregoing review asserts that in spite of the great efforts that existed in past works still significant improvements could be introduced as will be seen in the following section. These improvements aim to answer the following questions.

Could it be there a transverse velocity vertical profile that is very convenient for inclusion in analytical and numerical models without having complex logarithmic integral or infinite series functions? To answer that an equation will be provided for the vertical profile of the transverse velocity which has ordinary power functions without the complexity of the logarithmic integral or infinite series functions.

Could that velocity profile under fully developed flow conditions, be able to include effects of lateral surface wind forces and other surface forces? To answer that the developed transverse velocity equation has the capability of including lateral surface wind forces and other surface forces due to ship movements for example.

Could that velocity profile also allow for convenient derivation of the transverse-boundary shear stress? Unlike existing equations in the literature, the developed equation herein, due to its flexible power function structure, allows the evaluation of the derivative of the transverse velocity equation to evaluate the transverse boundary shear stress.

Could we find an expression for the boundary shear stress that balances all the forces including the centripetal and lateral pressure gradient forces? The developed expression for the transverse boundary shear includes both the centripetal and lateral pressure gradient forces.

Could a differentiation be made between the different deviation angles of the resultant flow velocity and the boundary shear? A differentiation will be made here between these two deviation angles as a separate expression will be developed for each type.

The following section will try to present answers to these important questions.

Materials and Methods

The present approach method rests on the integration of the transverse momentum equation, after making the necessary assumptions of steady and fully developed conditions, in the vertical direction and imposing the required boundary conditions. The boundary conditions include specifying the lateral shear stress force at the free surface and applying a condition of fully developed flow for the vertical profile of the transverse velocity. Evaluation of the derivative of the transverse velocity at the channel bed enables developing expression for the transverse boundary shear stress. Dividing the transverse bed velocity from the present approach by the longitudinal bed velocity results in expression for the deviation angle of the flow bed velocity while doing so for the transverse and longitudinal bed shear stresses provides an equation for the deviation angle of the bed shear stress. The equation for transverse velocity relies on two key assumptions. Firstly, it assumes a constant turbulent viscosity throughout the flow. Secondly, it relies on the condition that the topographic steering number is less than one, allowing for the approximation of mild curvature and meandering conditions.

DOI: 10.3844/ajessp.2024.1.21

Vertical Distribution of the Transverse Velocity

The starting point is to combine Eqs. (4 and 7) in the following form assuming incompressible flow, fully developed flow conditions, and constant eddy (turbulent) viscosity:

$$\frac{d}{dz}\left(\nu_T \frac{dv}{dz}\right) = g\, S_r - \frac{u^2}{r} \tag{31}$$

where, ν_T is assumed as a constant turbulent eddy viscosity.

In the context of turbulent flow in mildly meandering open channels, a constant turbulent eddy viscosity (ν_T) is assumed, which can be represented as $\nu_T = c\, U_* D$. In this way the turbulence is represented via the turbulent viscosity in terms of velocity scale (U_*) and length scale (D). As the size of the eddies and flow circulation in the cross-sectional plane of meandering channels is comparable to the channel depth, the channel depth thus can be considered as an appropriate length scale. In the meantime, the shear velocity represents the bed shear stress which generates turbulence thus making the shear velocity suitable velocity scale of turbulence. This approach of constancy of turbulent viscosity is supported by Molinas and Hafez (2000), who utilized a constant turbulent viscosity with c = 0.0765, as suggested by Laufer (1951) in their investigation of turbulent flow in a two-dimensional channel. Similar assumptions were also employed by Rastogi and Rodi (1978) in their study on heat and mass transfer in open channels. Notably, Molinas and Hafez (2000) successfully predicted the two-dimensional velocity field around vertical wall abutments by comparing their numerical model results with experimental data of Rajaratnam and Nwachukwu (1983); and Kheireldin (1995). Additionally, Talaa *et al.* (2002) achieved good agreement between their 2D numerical simulation of the heated side discharge problem and the experimental results of Makhail *et al.* (1975); Strazisar and Prahl (1973); and El-Ghorab (1999) by using a constant turbulent viscosity for flow and heat. It was shown by Hafez (1995) that detailed turbulence modeling is required for flows with corner effects and periodic wall roughness changes where the secondary currents are driven by the turbulence an-isotropy whereas the curvature-induced secondary currents herein are derived by the centripetal acceleration and transverse water surface slope, so turbulence is of secondary importance. Rodi (2000) extensively discussed the use of simplified turbulence models, highlighting their potential benefits. These simplified models, when applicable, offer computational efficiency, require less detailed input data, and involve fewer calibration parameters. Thangam and Speziale (1992); Hafez (1995) reported a large number of iterations for achieving convergence with their standard k-e turbulence model. However, simplified constant eddy viscosity models, such as those proposed by Tan (1992); Benque *et al.* (1982); Kimura and Hosoda (1997), require considerably fewer iterations to achieve convergence when solving engineering problems.

The assumption of constant turbulent viscosity is supported by previous studies and has been successfully applied in more complex turbulent flows such as jet flows (Talaa *et al.*, 2002), flows around abutments (Molinas and Hafez, 2000) and heat and mass (Rastogi and Rodi, 1978) further justifications are presented as follows. It will be demonstrated that the assumption of constant turbulent viscosity remains valid given the current state of knowledge.

Two options exist for modeling the turbulent viscosity profile: Utilizing the parabolic turbulent viscosity profile or employing a turbulence model such as the k-ε model. However, it is crucial to recognize that the nature of flow in the longitudinal and lateral channel directions is fundamentally different. In the longitudinal direction, the flow exhibits characteristics of free shear layer flow or typical boundary layer flow, where flow shear forces are balanced by boundary friction forces. On the other hand, the lateral direction involves circulatory flow governed by the centripetal, transverse water surface slope, and transverse boundary friction forces. Consequently, the turbulence structure and levels vary between the longitudinal and lateral directions. Therefore, the turbulent viscosity should ideally be anisotropic, depending on the flow directions. The parabolic turbulent viscosity, derived from longitudinal flow relations and which was utilized by Ascanio and Kennedy (1983) in their transverse velocity equation (Eq. (18) thereafter), may not accurately represent the turbulence structure in the cross-sectional direction of the meandering channel.

The constancy of a variable quantity is a common assumption in nearly all hydraulic studies. Roughness in alluvial channels changes from point to point due to variation in bed sediment grain sizes which in nature is not uniform. The Manning, Chezy and Darcy-Weisbach roughness equations which are some of the most used equations in hydraulic and hydrologic flow modeling assume constant roughness coefficient all over the whole cross-section. Almost all sediment transport bed load equations are one-dimensional adopting average or constant longitudinal velocity which also implies constant roughness. Even in two and three-dimensional flow models, the roughness coefficient is assumed constant within an element or grid cell. As elements or grid cells usually have dimensions in the order of meters when modeling natural alluvial channels, assuming constant roughness within an element becomes an approximating assumption of constancy in space. In addition, roughness and bed-load equations are developed under steady-state conditions and assumed applicable to unsteady conditions and this is also an approximating assumption but

DOI: 10.3844/ajessp.2024.1.21

constancy is assumed in time. The bottom line is that approximating assumptions have been always used in nearly all hydraulic studies so it is not uncommon to make an approximating assumption of constant turbulent viscosity keeping in mind that there is no other alternative considering the current state of knowledge. While it is recognized that these approximations have their limitations, it is crucial to acknowledge that alternatives to the assumption of constant turbulent viscosity are currently limited. Given the state of knowledge and the practical constraints in hydraulic studies, the assumption of constant turbulent viscosity remains a widely employed and justified approach. Researchers and practitioners continue to work towards improving these models and exploring alternative approaches, but in the absence of comprehensive alternatives, the assumption of constant turbulent viscosity remains a practical and reasonable choice.

The condition of the mildly curving and meandering channel is that the topographic steering number proposed by Hafez (2023) for delineation between mild and sharp bends is less than unity. The topographic steering number according to Hafez (2023) = $\frac{(r_2^{19} - r_1^{19})}{19\, r_c^{18}\, (r_2 - r_1)}$ where r_2 and r_1 are the outer and inner channel radius of curvature, respectively. This number is the ratio of the transverse energy slope loss in a sharp bend to that in a mild bend. When it is unity, it indicates that the condition in the considered bend is that of a mild bend.

Integrating Eq. (31) twice while solving for the transverse velocity yields:

$$v = \frac{1}{\nu_T}\left(\begin{matrix} g\, S_r\, \frac{z^2}{2} - \\ \frac{\bar{U}^2\,(p+1)^2}{r\, D^{2k}\,(2p+1)(2p+2)}\,(z)^{2p+2} \;+\; c_1\, z \end{matrix} \right) + \; c_2 \qquad (32)$$

Two boundary conditions are required to evaluate the two constants in Eq. (32). The first is at the water surface to specify the lateral surface shear stress or other surface forces and the second is for ensuring fully developed flow conditions. The first boundary condition at the surface could be expressed as:

$$\nu_T \left.\frac{\partial\, v}{\partial\, z}\right|_{z=D} = \; \pm\, \frac{\tau_{rs}}{\rho} \qquad (33)$$

where, τ_{rs} is the external radial surface shear stress acting on the water surface which could be due to the wind force or ship's lateral movement or any lateral surface forces and in the absence of these forces it could be assumed zero. It is noted that the ($\pm$) is inserted in front of the surface shear stress as the wind and also ship movement can be in either the inward or outward lateral directions. Applying Eqs. (32-33) and solving for c_1 yield:

$$c_1 = (-\, g\, S_r\, D + \frac{\bar{U}^2\,(p+1)^2}{r\,(2p+1)}\, D \pm \frac{\tau_{rs}}{\rho}) \qquad (34)$$

Substituting Eq. (34) for c_1 into Eq. (32) results in:

$$v = \frac{1}{\nu_T}\left(\begin{matrix} g\, S_r \left(\frac{z^2}{2} - \, D\, z\right) + \frac{\bar{U}^2\,(p+1)^2}{r\,(2p+1)} \\ \left(D\, z - \frac{Z^{2p+2}}{D^{2p}\,(2p+2)}\right) \pm \frac{\tau_{rs}}{\rho} z \end{matrix} \right) + \; c_2 \qquad (35)$$

It is noted from Eq. (35) that c_2 is equal to the lateral bed velocity, v_b, which is the lateral velocity at z = 0. It should be noted that the no-slip velocity boundary condition exists but it could be assumed to occur at the bottom of the immobile bed. It is the lower edge of the bed-load layer in which the sediment particles are assumed stationary or non-moving, i.e., at $z = -z_b$, v = 0, where z_b is the thickness or height of the bed-load layer. Therefore, it is understood herein that the theoretical bed lies at z = 0 with slip velocity which is the upper edge of the moving bed-load layer, and the zero velocity or no-slip velocity is assumed at the lower edge of the bed-load layer at $z = -z_b$.

Fully developed flow conditions along the vertical water column dictate that:

$$\int_0^D v\, dz = 0 \qquad (36)$$

Substituting Eq. (35) into Eq. (36) and integrating yield:

$$\left\{ \frac{1}{\nu_T}\left(\begin{matrix} g\, S_r \left(\frac{z^3}{6} - \, D\, \frac{z^2}{2}\right) + \frac{\bar{U}^2\,(p+1)^2}{r\,(2p+1)} \\ \left(D\, \frac{z^2}{2} - \frac{Z^{2p+3}}{D^{2p}\,(2p+2)\,(2p+3)}\right) \pm \frac{\tau_{rs}}{\rho}\frac{z^2}{2} \end{matrix} \right) + \; c_2 z \right\}\Bigg|_0^D = 0 \qquad (37)$$

Substituting the limits of integration in Eq. (37) and solving for c_2 yield:

$$v_b = \; c_2 = v|_{z=0} = \frac{1}{\nu_T}\left(\begin{matrix} g\, S_r \left(\frac{D^2}{3}\right) \\ -\, \frac{\bar{U}^2 D^2\,(p+1)\,(p+2)}{2\, r\,(2p+3)} \mp \frac{\tau_{rs}}{\rho}\frac{D}{2} \end{matrix} \right) \qquad (38)$$

It is emphasized that the radial velocity at the bed (v_b) is equal to the constant c_2. This allows Eq. (35) to be written as:

$$v = \frac{1}{\nu_T}\left(\begin{matrix} g\, S_r \left(\frac{z^2}{2} - \, D\, z\right) + \frac{\bar{U}^2\,(p+1)^2}{r\,(2p+1)} \\ \left(D\, z - \frac{Z^{2p+2}}{D^{2p}\,(2p+2)}\right) \pm \frac{\tau_{rs}}{\rho} z \end{matrix} \right) + \; v_b \qquad (39)$$

where, v_b is given as by Eq. (38).

The lateral surface velocity is given from Eq. (39) by substituting $z = D$ which results in:

$$v_s = \frac{1}{\nu_T}\left(-\, \frac{D^2}{2} g\, S_r + \frac{\bar{U}^2\,(p+1)\,D^2}{2\, r} \pm \frac{\tau_{rs}}{\rho} D\right) + \; v_b \qquad (40)$$

Equations (38-40) have the advantage that they include effects of the wind forces and forces due to lateral

DOI: 10.3844/ajessp.2024.1.21

ships' movement while these factors are absent in the existing transverse velocity profiles. They also have the most convenient form of being composed of power functions avoiding the complexity that could arise from the logarithmic or integral functions or power series that exist in Rozovskii (1961); Kikkawa *et al.* (1976); and Ascanio and Kennedy (1983).

Transverse Boundary Shear Stress

The transverse boundary or bed shear stress is given as:

$$\tau_{or} = \rho \nu_T \left.\frac{\partial v}{\partial z}\right|_{z=0} \quad (41)$$

It is noted from Eq. (32) that $\tau_{or} = \rho c_1$ which could be expressed according to Eq. (34) for c_1 as:

$$\tau_{or} = \rho D \left(\frac{\bar{U}^2 (p+1)^2}{r (2p+1)} - g S_r\right) \quad (42)$$

Equation (42) expresses that the transverse boundary shear stress balances the centripetal and the radial pressure forces unlike that in Eq. (30) by Ascanio and Kennedy (1983) who only considered balancing the centripetal force.

Flow Velocity and Boundary Shear Stress Deviation Angles

The surface velocity deviation angle, δ_{vs}, could be given according to Eq. (16) by substituting $z = D$ and with Eq. (40) yielding:

$$\tan\delta_{vs} = \frac{v_s}{u_s} = \frac{1}{\bar{U}(p+1)}\left(\begin{matrix} -\frac{D^2}{2\nu_T} g S_r + \\ \frac{\bar{U}^2 (p+1) D^2}{2 r \nu_T} \pm \frac{\tau_{rs}}{\rho \nu_T} D \end{matrix}\right) + \frac{v_b}{\bar{U}(p+1)} \quad (43)$$

In this study distinction is made between the near bed resultant flow velocity deviation angle and the resultant bed shear stress deviation angle as follows. The flow bed velocity deviation angle, δ_{vb}, using Eq. (38) for v_b, could be given as:

$$\tan\delta_{vb} = \frac{v_b}{u_b} = \frac{1}{u_b \nu_T}\left(\begin{matrix} g S_r \left(\frac{D^2}{3}\right) \\ -\frac{\bar{U}^2 D^2 (p+1)(p+2)}{2 r (2p+3)} \mp \frac{\tau_{rs}}{\rho} \frac{D}{2} \end{matrix}\right) \quad (44)$$

The resultant bed shear stress deviation angle, using Eq. (42) for τ_{or}, could be given as:

$$\tan\delta_{\tau b} = \frac{\tau_{or}}{\tau_{os}} = \frac{\rho \left(\frac{\bar{U}^2 (p+1)^2}{r (2p+1)} D - g S_r D\right)}{\rho \frac{\bar{U}^2 f}{8}} = \frac{8 \left(\frac{\bar{U}^2 (p+1)^2}{r (2p+1)} D - g S_r D\right)}{\bar{U}^2 f} \quad (45)$$

There are several ways for determining u_b appearing in Eq. (44) such as from the vertical distribution of the longitudinal main velocity or from a bed-load formula and the thickness of the bed-load layer. One way is to use the well-known logarithmic velocity distribution over the rough boundary which is given as:

$$\frac{u}{u_*} = 8.5 + 5.75 \log\left(\frac{z}{k_s}\right) \quad (46)$$

where, u_* is the local shear velocity, k_s is a representative roughness height of the bed surface. Assuming near the bed surface that $z = k_s$ results in an approximate value for the bed main velocity, u_b, as:

$$\frac{u_b}{u_*} \approx 8.5, \text{ or } u_b \approx 8.5\, u_*$$

Or more generally:

$$u_b \approx c_u u_* \quad (47)$$

where, c_u is a coefficient that depends on the flow conditions and it will be assumed herein as 8.5.

Alternatively, the deviation angle of the resultant boundary shear stress could be used for determining the deviation angle of the resultant flow velocity. The equation of the deviation angle for the resultant bed shear stress has much confidence due to knowledge with reasonable accuracy of the lateral and longitudinal boundary shear stresses. For the bed velocity deviation angle Eq. (44), the requirement of the longitudinal bed velocity as an input introduces some uncertainty. To overcome this it is assumed that the bed shear stress is proportional to the square of the flow bed velocity. The same proportionality would be assumed to be applicable to the deviation angle. It can be stated that: $\tan\delta_{\tau b} = \frac{\tau_{or}}{\tau_{os}} \approx \frac{\rho {v_b}^2}{\rho {u_b}^2} = \frac{{v_b}^2}{{u_b}^2} = (\tan\delta_{vb})^2$. Thus it can be assumed the bed velocity angle is proportional to the square root of the boundary shear stress angle as:

$$\tan\delta_{vb} = \sqrt{\tan\delta_{\tau b}} = \sqrt{\frac{8 \left(\frac{\bar{U}^2 (p+1)^2}{r (2p+1)} D - g S_r D\right)}{\bar{U}^2 f}} \quad (48)$$

where, $(\tan\delta_{\tau b})$ is given as by Eq. (45). Comparing Eq. (48 and 24), it can be seen that Eq. (48) has the advantage of including the main velocity and roughness effects which are absent in Eq. (24). It should be noted that Eq. (24), in spite of its wide use, is based on the transverse velocity for smooth beds while natural rivers have rough beds.

Methods for Evaluation of the Developed Equations

Transverse velocity data exist but, unfortunately, the bends might be either very sharp bends as curved laboratory channels of a *U* shape with a central angle of 180°, or no measurements of the vertical distribution of the transverse velocity, or no reporting data exist for the roughness conditions of the curved channel (Blanckaert, 2010; Pradhan *et al.*, 2018; Bai *et al.*, 2019; He *et al.*, 2021).

DOI: 10.3844/ajessp.2024.1.21

To evaluate the accuracy of the developed equation for transverse velocity and in the absence of existing data to do that, we conducted tests using a hypothetical channel. The channel had a Manning's roughness coefficient of 0.013, a width of 10 m, a depth of 2.0 m, a slope of 0.0001, and a channel center line radius of curvature of 50 m. Based on these parameters, the average longitudinal velocity was determined to be 0.976 m/s, with a flow discharge of 19.51 m^3/s. The friction factor was found to be 0.0118 and the corresponding Chezy's coefficient indicated a smooth bed roughness of 81.6. To investigate roughness effects, additional values of Manning's roughness coefficients of 0.025 and 0.05 were taken.

For the analysis, we assumed a rectangular channel with substantial width, where the depth-averaged velocity was considered equal to the cross-sectional average velocity. Additionally, the depth-averaged shear velocity (u^*) was approximated as equal to the cross-sectional shear velocity (U^*). The depth-averaged turbulent viscosity was calculated when using Eq. (39) as $u^* D/15 \approx 0.067\, u^* D$, which represents the depth-averaged value of the widely recognized parabolic turbulent viscosity vertical distribution proposed by Fischer *et al*. (1979) as $\nu_T = \kappa u_* z\,(1 - z/D)$.

Finally, we address the influence of lateral surface forces, such as lateral wind shear stress. As an illustrative example, we consider the cross-section and hydraulic data of Muddy Creek, Wyoming, as reported by Dietrich and Smith (1983). Unfortunately, no wind-induced transverse velocity data were available in the literature for direct comparison with our approach. To the best of our knowledge, such data for transverse velocity in meandering channels are currently unavailable. For the Muddy Creek case, the mean water depth, width, depth-averaged velocity, discharge, longitudinal water surface slope, and river centreline radius of curvature were determined as 0.40 m, 4.0 m, 0.55 m/s, 1.1 m^3/s, 0.0014 and 8.0 m, respectively. In our analysis, we assumed lateral wind blowing inward or outward with a wind shear stress of 0.5 Pa. This value corresponds to a wind speed of 10 m/s, assuming an air density of 1.2 kg/m^3 and a drag coefficient of 0.0042.

Results

Table 1 presents the results obtained by applying Eqs. (13, 19, 22 and 39) with Manning's roughness coefficients of 0.013 and 0.025 to calculate the vertical profile of the transverse velocity. Figures 3-5 depict the lateral velocity profiles for different roughness values: 0.013, 0.025, and 0.05, respectively. Figures 6-7 illustrate the effects of varying Manning's roughness coefficients on the transverse surface velocity and the transverse bed velocity, respectively, using the same hydraulic data as the previous examples. The Manning's roughness coefficient varied incrementally from 0.01-0.1 to cover a wide range of values observed in natural channels. Figure 8 demonstrates the variation of transverse boundary shear stress with respect to Manning's roughness coefficient, while Fig. 9 shows the deviation angle of the boundary shear stress as a function of channel roughness. Figure 10 illustrates the effects of inward and outward wind shear stress of 0.5 Pa on the vertical profile of the transverse velocity when the comparison is made against the no-wind profile.

Table 1: Vertical profiles for the transverse velocity (m/s) using different analytical equations for Manning's roughness (n) = 0.013 and 0.025

	Transverse velocity (m/s) for n = 0.013				Transverse velocity (m/s) for n = 0.025			
z/D	Eq. (13)	Eq. (19)	Eq. (22)	Eq. (39)	Eq. (13)	Eq. (19)	Eq. (22)	Eq. (39)
1.00	0.315	0.348	0.315	0.328	0.159	0.173	0.159	0.171
0.95	0.311	0.314	0.283	0.324	0.157	0.155	0.143	0.169
0.90	0.301	0.279	0.252	0.313	0.151	0.138	0.127	0.163
0.85	0.284	0.244	0.220	0.295	0.143	0.121	0.111	0.154
0.80	0.261	0.209	0.189	0.271	0.131	0.104	0.095	0.141
0.75	0.232	0.174	0.157	0.241	0.116	0.086	0.079	0.125
0.70	0.199	0.139	0.126	0.207	0.099	0.069	0.063	0.107
0.65	0.161	0.105	0.094	0.167	0.079	0.052	0.048	0.086
0.60	0.119	0.070	0.063	0.123	0.058	0.035	0.032	0.063
0.55	0.073	0.035	0.031	0.076	0.035	0.017	0.016	0.038
0.50	0.025	0.000	0.000	0.027	0.011	0.000	0.000	0.012
0.45	-0.025	-0.035	-0.031	-0.025	-0.014	-0.017	-0.016	-0.014
0.40	-0.076	-0.070	-0.063	-0.078	-0.040	-0.035	-0.032	-0.042
0.35	-0.127	-0.105	-0.094	-0.131	-0.065	-0.052	-0.048	-0.069
0.30	-0.177	-0.139	-0.126	-0.183	-0.090	-0.069	-0.063	-0.096
0.25	-0.226	-0.174	-0.157	-0.234	-0.114	-0.086	-0.079	-0.121
0.20	-0.272	-0.209	-0.189	-0.281	-0.136	-0.104	-0.095	-0.145
0.15	-0.312	-0.244	-0.220	-0.324	-0.155	-0.121	-0.111	-0.167
0.10	-0.347	-0.279	-0.252	-0.361	-0.171	-0.138	-0.127	-0.186
0.05	-0.371	-0.314	-0.283	-0.389	-0.182	-0.155	-0.143	-0.200
0.00	-0.382	-0.348	-0.315	-0.404	-0.187	-0.173	-0.159	-0.209

DOI: 10.3844/ajessp.2024.1.21

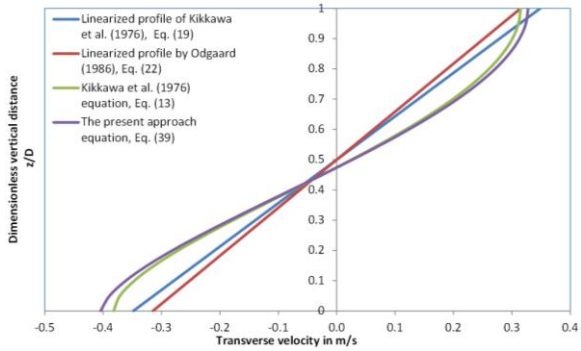

Fig. 3: Vertical profiles for the transverse velocity using different analytical equations for n = 0.013

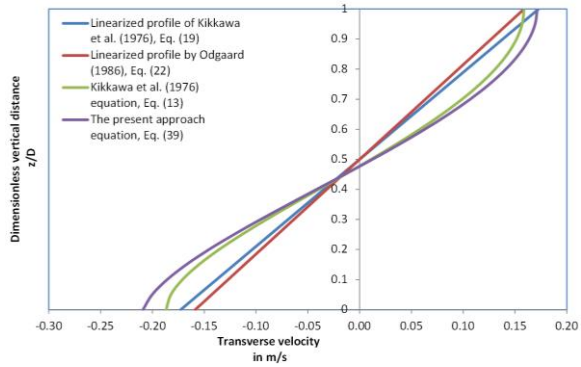

Fig. 4: Vertical profiles for the transverse velocity using different analytical equations for n = 0.025

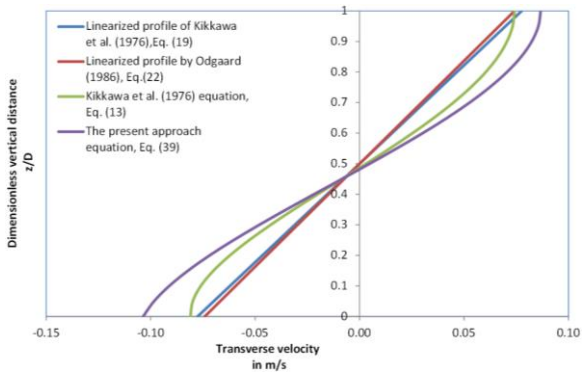

Fig. 5: Vertical profiles for the transverse velocity using different analytical equations for n = 0.05

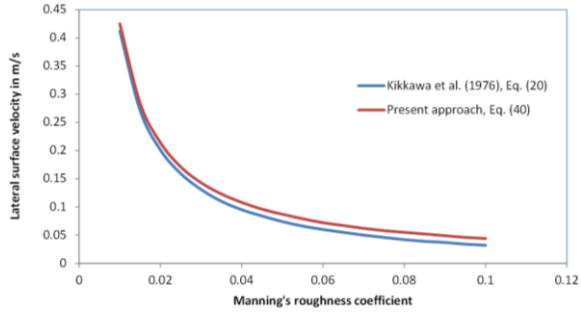

Fig. 6: Effects of Manning's roughness coefficient on the lateral surface velocity

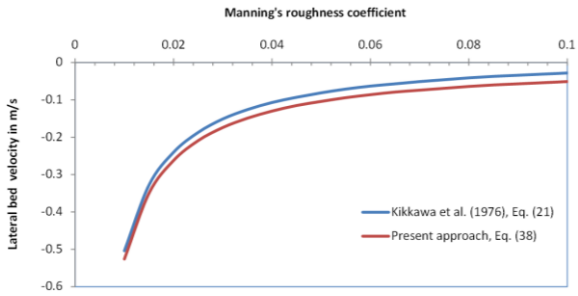

Fig. 7: Effects of Manning's roughness coefficient on the lateral bed velocity

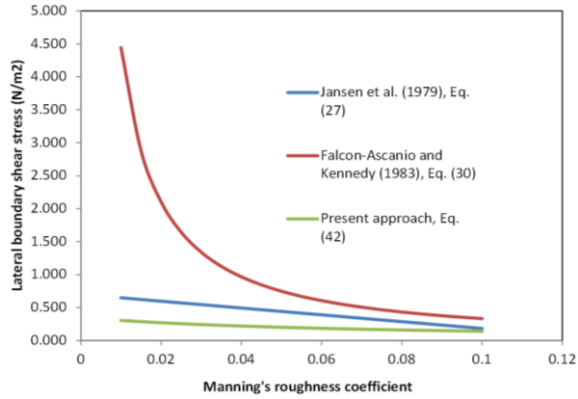

Fig. 8: Variation of the transverse-boundary shear stress versus Manning's roughness coefficient.

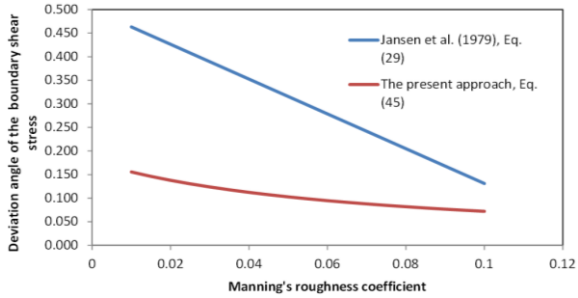

Fig. 9: Deviation angle of the boundary shear stress variation against channel roughness

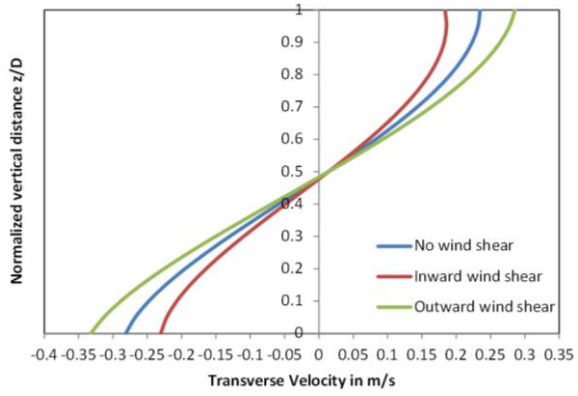

Fig. 10: Effects of inward and outward wind shear stress of 0.5 Pa on the transverse velocity vertical profile

Table 2: Effects of roughness on the surface flow velocity deviation angle

Manning's roughness coefficient (n)	Surface Velocity deviation angle from Eq. (43) in radians	Surface velocity deviation angle from Eq. (43) in degrees
0.001	0.312	17.3
0.015	0.303	16.8
0.002	0.294	16.4
0.025	0.285	15.9
0.003	0.277	15.5
0.035	0.270	15.1
0.004	0.263	14.7
0.045	0.256	14.4
0.005	0.250	14.0
0.055	0.243	13.7
0.006	0.238	13.4
0.065	0.232	13.1
0.007	0.227	12.8
0.075	0.222	12.5
0.008	0.217	12.2
0.085	0.212	12.0
0.009	0.208	11.8
0.095	0.204	11.5
0.001	0.200	11.3

Table 2 presents the effects of roughness on the surface flow deviation angle, while Table 3 examines the impact of bed roughness on the deviation angle of the near-bed resultant flow velocity. Additionally, Table 4 compares the deviation angles for the resultant flow velocity (Eq. 48) and the resultant boundary shear stress (Eq. 45) against channel roughness.

Discussion

In the discussion section, we thoroughly analyze the applications of the present approach and compare them with the equations derived from previous methods, as presented in the results section. Figure 3, for the case of n = 0.013, illustrates the similarity between the two linear profiles in Eq. (19) according to Kikkawa *et al*. (1976) and Eq. (22) according to Odgaard (1986a), while the two nonlinear profiles in Eq. (13) by Kikkawa *et al*. (1976) and Eq. (39) by the present approach also exhibit close resemblance, albeit with noticeable differences, particularly at the bed and surface levels. This indicates that the straight-line approximation is not entirely accurate, especially at the bed. Furthermore, the two linear profiles are zero at mid-depth, while the two nonlinear profiles deviate from zero at that point. It is worth noting that the velocities predicted by Eq. (39) are slightly higher than those predicted by Eq. (13) throughout the entire depth, especially at the bed.

In Fig. 4, for the case of n = 0.025, the overall trend is similar to that observed for n = 0.013, except that the differences at the channel bed become more pronounced, with the velocity predicted by Eq. (39) being the highest. As roughness increases (n = 0.05), Fig. 5 demonstrates significant discrepancies between Eq. (39) of the present approach and the remaining equations, which coincide with each other. For instance, Eq. (39) predicts a lateral surface velocity of 0.087 m/s, whereas Eq. (13) by Kikkawa *et al*. (1976) predicts 0.074 m/s, resulting in an absolute relative difference of 17.6%. Similarly, for the lateral bed velocity, Eq. (39) predicts -0.104 m/s, while Eq. (13) predicts -0.081 m/s, with an absolute relative difference of 28.4%.

Considering that the phenomenon of secondary currents in meandering channels is inherently nonlinear, as indicated by the governing flow equations, it can be inferred that the nonlinear Eq. (13) by Kikkawa *et al*. (1976) and Eq. (39) by the present approach) provide a more accurate representation compared to the linear ones. Comparing the present approach Eq. (39) with that of Kikkawa *et al*. (1976), it can be concluded that the present approach performs better based on the results presented in Figs. 3-5, as well as Table 1, for several reasons. Firstly, the present approach equation exhibits sensitivity to channel bed roughness, while in Kikkawa *et al*. (1976) equation, the tangent line or derivative of the transverse velocity profile at the bed, which is related to the transverse boundary shear stress, appears to be very high or nearly vertical, indicating an extremely large or infinite transverse boundary shear stress. In contrast, the present approach equation shows a finite slope of the tangent line at the bed, which is more realistic for roughness values commonly observed in meandering channels. Furthermore, at a Manning roughness of 0.05, which is close to the roughness values found in meandering channels, Kikkawa *et al*. (1976) equation coincide with the linear velocity profile, as illustrated in Fig. 5. Additionally, the present approach equation yields higher bed and surface transverse velocities than the equation proposed by Kikkawa *et al*. (1976), which ensures a more conservative estimation when considering the effects of transverse velocity on bank erosion and point-bar formation.

It is important to note, as evident from Table 1, Figs. 3-5, that the lateral bed velocity predicted by the present approach Eq. (39) is higher than the lateral surface velocity. This disparity arises due to the enforcement of fully developed flow conditions by the present approach, as demonstrated by Eq. (36). The transverse velocity is influenced by two mechanisms: The constant transverse water slope force and the centripetal force, which varies along the depth due to the nonlinear profile of the u velocity. The constancy of the transverse water surface slope force causes the lateral bed velocity to surpass the lateral surface velocity, as its effect extends throughout the entire depth, unlike the centripetal force, which diminishes when moving closer to the bed surface. However, this observation does not impact the calculation of the transverse boundary shear stress, which is obtained via Eq. (41), irrespective of the boundary condition used for the lateral velocity, whether it is a no-slip condition or the enforcement of fully developed conditions using

Eq. (36). The lateral boundary shear stress affects the transverse bed slope and the transverse bed-load transport. Therefore, the equations developed for these parameters, based on the developed equation for the lateral boundary shear, remain independent of the lateral velocity boundary condition specified in Eq. (36).

Notably, all the Eqs. (13, 19, 22 and 39) exhibit an increase in lateral velocity and, consequently, the strength of the secondary currents with an increase in the ratio of the depth to centreline curvature radius (*D/r*) or a decrease in *r/D*. This observation aligns with the findings of three experiments conducted by Li *et al*. (2022) under different flood frequencies, which investigated the influence of the *r/D* ratio on the distribution and characteristics of secondary flow, turbulence, and momentum transport using acoustic Doppler velocimetry. The experiments revealed that the intensity of the secondary flow decreased as the value of *r/D* increased. This finding is consistent with Eq. (39) and supports the previous equations, which indicate a decrease in transverse velocity with increasing *r*/*D*.

It should be noted that the data in Fig. (2) include the dimensionless transverse velocity against the dimensionless vertical distance without specifying many necessary flow parameters such as the longitudinal depth-average velocity, the channel radius of curvature, and the roughness coefficient. This precluded using the data in Fig. (2) for comparison purposes. In addition, published experimental data are typically for very sharp meander bends with a 180° central bend angle while the approach is for mild bends which often exist in nature. In the meantime as Odgaard (1986a) stated that his linear transverse velocity equation is in good agreement with the data in Fig. (2), it is seen that comparison of the present approach equation to this linear equation and to the other past equations, which are also tested against data, is the best possible way for testing the developed equation. This is similar in mathematics to the well-known transitive property: If A is similar to B and B is similar to C, then A is similar to C.

Figure 6 illustrates the impact of roughness, represented by variations in Manning's roughness coefficient, on the transverse surface velocity according to Kikkawa *et al*. (1976) (Eq. 20) and the present approach (Eq. 40), while disregarding the surface shear stress caused by wind. At a low roughness value of n = 0.01, the lateral surface velocity ratio of the present approach to Kikkawa *et al*. (1976) is 1.03. This ratio increases to approximately 1.20 at $n = 0.06$, indicating a 20% increase, and further rises to 1.38 at $n = 0.1$, representing a 38% increase. Both equations exhibit a steep decrease in surface velocity as roughness increases until approximately $n \approx 0.04$, after which the velocity profiles tend to flatten. The lateral surface velocity is of great importance due to its influence on bank erosion and lateral meander migration. Thus, from a design perspective of bank erosion protection works, the present approach equation is considered to be more conservative and safer than Kikkawa *et al*. (1976) equation. It is worth noting that both equations assume a constant turbulent viscosity.

In Fig. 7, the effect of roughness variation represented by Manning's roughness coefficient on the transverse bed velocity is shown for Kikkawa *et al*. (1976) Eq. (21) and the present approach Eq. (38), while neglecting the surface wind shear stress. At a low roughness value of n = 0.01, the ratio of the present approach to Kikkawa *et al*. (1976) lateral bed velocity is 1.04. This ratio increases to about 1.36 at n = 0.06, indicating a 36% increase. The difference becomes highly significant at n = 0.1, where the ratio reaches 1.81, representing an approximately 81% increase. The lateral bed velocity is crucial due to its effects on the transverse bed slope, transverse sediment movement, and point-bar formation. Thus, considering the influence of lateral bed velocity on the transverse bed slope and lateral sediment transport, the present approach equation is considered to be more conservative and safer than Kikkawa *et al*. (1976) equation.

Table 2 presents the influence of channel bed roughness, represented by Manning's roughness coefficient (*n*), on the deviation angle of the surface flow velocity, as given by Eq. (43) in the present approach. It is evident that roughness has a dampening effect on the deviation angle, with the surface flow deviation angle being 17.3 degrees at n = 0.01. As roughness increases, the deviation angle decreases to 13.4 degrees at n = 0.06 and further decreases to 11.3 degrees at n = 0.1, representing a significant 35% decrease. The surface flow transverse velocity is important in determining the flow attacking angle of the outer bank that influences bank scour.

Moving to Table 3, it can be observed that at a low roughness value of n = 0.01, the flow bed-velocity deviation angle, computed using Eq. (44) in the present approach, reaches approximately 59 degrees. However, as roughness increases, the deviation angle starts to decrease and reaches 9.1 degrees at a high roughness value of n = 0.1. This small deviation angle indicates that the resultant bed velocity becomes nearly parallel to the channel axis direction. It should be noted that Eq. (24) by Rozovskii (1961) provides a deviation angle, independent of bed roughness, of 23.7 degrees. This corresponds to the prediction made by Eq. (44) in the present approach for roughness coefficients between 0.035 and 0.040. As expected, the range of deviation angles for the bed velocity is much broader compared to the surface velocities, primarily due to the significant influence of channel bed roughness on bed velocities. Furthermore, since the energy slope was kept constant in the considered hypothetical channel, the bed velocity remained consistent across all values of the roughness coefficient, owing to the constancy of the shear velocity. The flow bed-velocity deviation angle highly influences sediment movement along the bed transverse slope and point-bar formation.

DOI: 10.3844/ajessp.2024.1.21

Table 3: Effects of roughness on the flow bed-velocity deviation-angle

Manning's roughness coefficient (n)	Average main velocity in m/s	Lateral bed velocity in m/s	Longitudinal bed velocity in m/s	Bed velocity deviation angle from Eq. (44) in radians	Bed velocity deviation angle from Eq. (44) in degrees
0.001	1.268	-0.526	0.318	1.653	58.8
0.015	0.846	-0.350	0.318	1.100	47.7
0.002	0.634	-0.262	0.318	0.823	39.5
0.025	0.507	-0.209	0.318	0.657	33.3
0.003	0.423	-0.174	0.318	0.547	28.7
0.035	0.362	-0.149	0.318	0.468	25.1
0.004	0.317	-0.130	0.318	0.408	22.2
0.045	0.282	-0.115	0.318	0.362	19.9
0.005	0.254	-0.104	0.318	0.326	18.0
0.055	0.231	-0.094	0.318	0.296	16.5
0.006	0.211	-0.086	0.318	0.271	15.1
0.065	0.195	-0.079	0.318	0.249	14.0
0.007	0.181	-0.074	0.318	0.231	13.0
0.075	0.169	-0.069	0.318	0.215	12.2
0.008	0.159	-0.064	0.318	0.202	11.4
0.085	0.149	-0.060	0.318	0.190	10.7
0.009	0.141	-0.057	0.318	0.179	10.1
0.095	0.134	-0.054	0.318	0.169	9.6
0.001	0.127	-0.051	0.318	0.161	9.1

In summary, Table 2 demonstrates the dampening effect of roughness on the deviation angle of surface flow transverse velocity. As roughness increases, the deviation angle decreases, indicating a more aligned flow with the channel axis. Similarly, Table 3 highlights the relationship between roughness and the deviation angle of bed velocities. Higher roughness values are associated with smaller deviation angles, implying a flow that is more parallel to the channel axis. These findings emphasize the significant influence of roughness on both surface and bed velocities, with the former being less affected due to the constancy of shear velocity.

Figure 8 illustrates the variation of lateral boundary shear stress against roughness. It is evident that Eq. (30) by Ascanio and Kennedy (1983) predicts significantly higher values compared to Eq. (27) by Jansen *et al.* (1979) and Eq. (42) from the present approach. The higher values predicted by Eq. (30) can be attributed to its omission of the contribution of the transverse water surface, which plays a significant role in balancing the centripetal force. It should be noted that while Eqs. (27 and 42) exhibit a nearly straight line form, and Eq. (30) follows a descending curve-like shape. However, at high roughness values, the three equations converge and the differences become smaller. Due to the omission of the contribution from the transverse water surface, Eq. (30) can be excluded from the comparison. Unfortunately, a direct comparison between Eqs. (27 and 42) is not possible due to the unavailability of data.

Figure 9, presents the deviation angle of the resultant bed shear stress from the channel axis according to Eq. (29) by Jansen *et al.* (1979) and Eq. (45) from the present approach. It is evident that the values predicted by Eq. (29) are significantly higher than those of Eq. (45). At n = 0.01, Eq. (29) predicts deviation angles approximately three times higher than Eq. (45) and this ratio decreases to about two times at n = 0.1. In terms of deviation angles in degrees, Eq. (29) predicts angles of 24.8 degrees, 19.4 degrees, and 7.4 degrees at n = 0.01, 0.04 and 0.1, respectively. On the other hand, Eq. (45) predicts deviation angles of 8.8 degrees, 6.4 degrees, and 4.1 degrees at the same roughness coefficients, respectively. Similar to the previous case, a direct comparison between Eqs. (29 and 45) is not possible due to the unavailability of data.

To summarize, Fig. 8 demonstrates that Eq. (30) overestimates the lateral boundary shear stress due to its omission of the contribution from the transverse water surface. While Eqs. (27 and 42) show different shapes, they converge at higher roughness values. Unfortunately, a direct comparison between Eqs. (27 and 42) was not feasible due to data limitations. Equation (29) predicts significantly higher bed-shear stress angles compared to Eq. (45) according to Fig. 9, indicating the influence of the choice of the equation on the estimated deviation angles. However, a direct comparison between Eqs. (29 and 45) could not be made due to the unavailability of data.

Table 4 provides valuable insights into the deviation angles of the resultant flow velocity, as determined by Eq. (48), and the boundary shear stress, as calculated using Eq. (45). It is evident that the deviation angle for the resultant flow velocity is higher than that of the boundary shear stress and both exhibit a consistent decreasing trend with increasing channel roughness.

DOI: 10.3844/ajessp.2024.1.21

Table 4: Deviation angles for the resultant bed shear, and flow velocity

Manning's roughness coefficient (n)	Resultant bed shear deviation angle from Eq. (45) in degrees	Resultant flow velocity deviation angle from Eq. (48) in degrees	$\tan \delta_{\tau b}$ from Eq. (45) (dimensionless)	$\tan \delta_{vb}$ from Eq. (48) (dimensionless)
0.001	8.8	21.5	0.156	0.394
0.015	8.3	20.9	0.146	0.382
0.002	7.9	20.4	0.138	0.371
0.025	7.4	19.9	0.130	0.361
0.003	7.1	19.4	0.124	0.352
0.035	6.7	18.9	0.118	0.343
0.004	6.4	18.5	0.112	0.335
0.045	6.1	18.1	0.107	0.328
0.005	5.9	17.8	0.103	0.321
0.055	5.6	17.4	0.099	0.314
0.006	5.4	17.1	0.095	0.308
0.065	5.2	16.8	0.091	0.302
0.007	5.0	16.5	0.088	0.296
0.075	4.8	16.2	0.085	0.291
0.008	4.7	16.0	0.082	0.286
0.085	4.5	15.7	0.079	0.281
0.009	4.4	15.5	0.077	0.277
0.095	4.3	15.3	0.074	0.273
0.001	4.1	15.0	0.072	0.269

Notably, at a low roughness value of approximately n = 0.01, the deviation angle for the resultant flow velocity is comparable to arctan (11 *D/r*), which is approximately 23.8 degrees according to Eq. (24) by Rozovskii (1961). This indicates that Eq. (24) does not account for the effects of roughness, while the present approach, represented by Eq. (48), takes roughness into consideration.

In the range of roughness values commonly observed in natural river channels, such as n between 0.025 and 0.045, the deviation angle of the velocity ranges from about 20 degrees to 18 degrees. This further supports the notion that Eq. (24) fails to incorporate the influence of roughness, whereas Eq. (48) in the present approach adequately considers roughness effects.

To summarize, Table 4 highlights that the deviation angle of the resultant flow velocity, as determined by Eq. (48), exceeds that of the boundary shear stress calculated using Eq. (45), while both angles decrease as channel roughness increases. The comparison with Eq. (24) by Rozovskii (1961) emphasizes that Eq. (24) overlooks roughness effects, whereas Eq. (48) in the present approach appropriately accounts for roughness.

The approach employed in the present study utilizes the logarithmic law of velocity distribution to compute the near-bed main or longitudinal velocity while assuming the power law to be applicable throughout the depth in the transverse velocity equation, as represented by the term u^2/r. This choice can be explained as follows:

It is widely recognized that the power law velocity profile is consistent with experimental observations in the outer 90% of the boundary layer, typically in the range of $0.1 < z/D < 1.0$, as established by Roberson and Crowe (1985). In this region, the power law accurately represents the velocity distribution.

On the other hand, the logarithmic law of velocity distribution is valid near the wall for values of zu^*/v (where v is the kinematic viscosity) ranging from approximately 30-500. Therefore, it is employed to accurately determine the near-bed main velocity.

In the transverse velocity equation, the contribution of the longitudinal velocity is represented by the term u^2/r, which corresponds to the centripetal acceleration. Near the bed, the main velocity (u) is relatively small, resulting in a further decrease in the term u^2/r due to squaring the near-zero velocity. Consequently, the main velocity near the bed has minimal significance in terms of its influence on the transverse velocity distribution. However, when calculating the near-bed main velocity itself, the logarithmic distribution becomes important and is utilized to accurately capture the velocity near the bed.

In summary, the present approach combines the logarithmic law of velocity distribution to compute the near-bed main velocity and the power law to describe the transverse velocity distribution. This choice is supported by the applicability of the power law in the outer boundary layer and the validity of the logarithmic law near the wall. While the main velocity near the bed has a limited impact on the transverse velocity distribution, it is crucial to accurately determine the near-bed main velocity using the logarithmic distribution.

Equation (48) offers a distinct advantage over Eq. (44) in that it does not require knowledge of the near-bed velocity, which can be a challenging task to obtain accurately. This advantage is significant because

DOI: 10.3844/ajessp.2024.1.21

acquiring precise information about near-bed velocity can be difficult in practice.

When comparing the predictions of Eqs. (44 and 48) for the resultant flow velocity deviation angle, it is apparent that the angles predicted by the latter equation exhibit a narrower range, ranging from 21.5-15.0 degrees. In contrast, the range of angles predicted by Eq. (44) spans from 58.8-9.1 degrees. This indicates that Eq. (48) provides more consistent and constrained results for the deviation angles.

Both Eqs. (44 and 48) have an advantage over Eq. (24) in that they account for the effects of main velocity and roughness, which are crucial factors in flow and sediment investigations. The inclusion of these factors is essential for accurate modeling and testing purposes. However, the suitability of each equation for specific applications should be determined through testing and comparison with available data.

It is worth noting that both Eqs. (44 and 48) can be utilized in equations such as the one proposed by Bridge (1977) for transverse bed slope and the equation presented by Parker (1984) for bed-load deviation angle. These equations, which rely on the inclusion of main velocity and roughness effects, can benefit from the use of either Eqs. (44 or 48), depending on the specific requirements and available data.

In conclusion, Eq. (48) offers an advantage over Eq. (44) by not relying on near-bed velocity information. The deviation angles predicted by Eq. (48) exhibit a narrower range compared to Eq. (44). Both Eqs. (44 and 48), incorporate main velocity and roughness effects, thus providing an improvement over Eq. (24). The suitability of each equation should be evaluated based on empirical testing and comparison with relevant data. These equations can be applied in various sediment and flow investigations, including equations proposed by Bridge (1977); Parker (1984).

It is important to recognize that the present approach primarily focuses on one-dimensional analysis, where the equation of motion in the lateral direction (Eq. 4) is integrated vertically along the z-axis. There are several cases where comprehensive analyses in the stream-wise and transverse directions require knowledge of the fully developed transverse velocity profile as a boundary condition. For instance, meander-path models like those proposed by Chang (1984); Odgaard (1986b) rely on accurate transverse velocity profiles. Similarly, in analyses involving the lateral direction (r), such as calculating lateral depth and sediment grain size distributions as in Bridge (1977); Odgaard (1984; 1986a-b), equations integrated in the vertical direction (z) have been utilized. This suggests that the developed equations in this study can be valuable in analyses related to the streamwise and transverse directions.

Similarly, a quasi-nonlinear approach can be employed, assuming mild curvature conditions ($R_c >> B$) and that the topographic steering number is less than 1, which allows for neglecting second-order terms (e.g., velocity combinations like (u, v), (u, w), (v, w)). It should be noted that the characterization of mild curvature condition via the condition $R_c >> B$ has no definitive limit or quantitative characteristics while the topographic steering number criterion offers such definitive and quantitative characterization. This simplifies the equations of motion significantly, as demonstrated in Eqs. (3-4). The resulting equations involve the local flow depth and the local depth-averaged velocity, both of which may vary with the radial direction (r). Consequently, integration of these resulting equations with respect to r becomes feasible by utilizing relations for the lateral variations of $D(r)$ and $U(r)$, assuming a topographic steering condition as discussed in Blanckaert (2010); Hafez (2023).

In summary, while the present approach primarily focuses on one-dimensional analysis, it is noteworthy that the developed equations can be applied to analyses involving the streamwise and transverse directions. Additionally, a quasi-nonlinear approach can be adopted by neglecting second-order terms under mild curvature conditions, resulting in simplified equations that depend on the radial direction. The integration of these equations is facilitated by considering lateral variations of flow depth and depth-averaged velocity, which can be achieved through a topographic steering condition as discussed in Hafez (2023).

Figure (10) provides valuable insights into the impact of inward and outward wind shear stress on the transverse velocity vertical profile for a wind shear stress of 0.5 Pa. This value, of the wind shear stress, amounts to a wind speed of 10 m/s, while an air density of 1.2 kg/m^3 and a drag coefficient of 0.0042 are assumed. At the water surface, the transverse surface velocity is calculated at 0.23 m/s in the absence of wind stress. However, when the wind stress is directed inward, opposing the centripetal force, the transverse surface velocity decreases to 0.18 m/s. Conversely, when the wind stress is directed outward, aligned with the centripetal force, the transverse surface velocity increases to 0.29 m/s. These changes in transverse velocity due to wind stress correspond to significant percentage variations, with a 22% decrease observed for inward wind stress and a 26% increase for outward wind stress.

Furthermore, the effect of wind stress on transverse bed velocity is noteworthy. It is observed that the decrease in transverse bed velocity matches the increase in transverse surface velocity, resulting in an 18% percentage change. This symmetry in the effects of wind stress on the transverse velocity at the surface and bed highlights the important role of wind stress in influencing these variables.

DOI: 10.3844/ajessp.2024.1.21

Notably, if the outward wind shear stress is halved to a value of 0.25 Pa (equivalent to a wind speed of approximately 7 m/s), the increase in transverse surface velocity is reduced to 13% and the increase in transverse bed velocity is reduced to 11%. This demonstrates the sensitivity of transverse velocities to variations in wind stress and underscores the significance of accurately measuring wind data in field studies. Accounting for wind stress effects on velocity and other dependent variables is crucial in order to understand and interpret field data accurately. It also elucidates potential differences observed between laboratory and field data, as wind effects can contribute to such discrepancies.

In summary, Fig. (10) provides compelling evidence of the influence of wind shear stress on the transverse velocity profile. It illustrates significant changes in transverse velocities at the water surface and bed due to inward and outward wind stress. The data highlights the importance of considering wind stress effects by accurately measuring wind data in field studies. The profile comparison in Fig. (10) further demonstrates that the no wind velocity profile lies between the profiles corresponding to inward and outward wind directions.

Table (5) offers a valuable comparison between previously developed transverse velocity equations and the equation derived in the present study. The results clearly indicate that the transverse velocity equation proposed in this approach, Eq. (39), outperforms the other equations in terms of practicality, ease of use, mathematical simplicity, and its construction using ordinary power functions. Moreover, Eq. (39) enables the calculation of transverse bed velocity and transverse boundary shear stress and allows for the incorporation of lateral forces such as wind and ship movements.

The implications of the proposed approach and the derived equations are significant in the field of river engineering and management. By considering lateral forces induced by wind and ship movements, the characterization of flow in meandering channels becomes more accurate and comprehensive. This enhanced understanding of flow behavior can inform the design and maintenance of river systems, particularly in regions where wind and ship activities play a vital role.

As an alternative to the adoption of a constant turbulent viscosity, applying a turbulence model such as the two-equation k-ε model necessitates solving for the flow velocity field first; which is then used as an input for the turbulence model. However, this sequential solution process introduces challenges. Two boundary conditions are required to solve for the transverse momentum equation, such as Eq. (2). At the free surface, either a zero shear stress condition or a specified shear stress due to wind can be specified. At the bottom, two options exist, both related to the transverse velocity at the boundary. The first option is the no-slip velocity condition, but it requires knowledge of the thickness of the transverse bed load layer, which has not been fully developed yet. The second option is to specify the transverse bed velocity at the top edge of the transverse bed load layer (movable boundary velocity condition or virtual wall function boundary condition approach as in Hafez (1995), which is typically unknown. Hence, the system remains unclosed, and certain assumptions must be made.

Considering the challenges associated with solving the transverse velocity field and the dependence of turbulent viscosity on the unknown transverse bed velocity, the assumption of constant turbulent viscosity can be adopted as a first approximation. Since assumptions are necessary and the ability to determine which assumption is superior is limited, the assumption of constant turbulent viscosity provides a reasonable starting point. In fact, knowledge of the transverse bed velocity, which can be provided by the present approach, is required to determine the turbulent viscosity field. Therefore, neither a reliable nor accurate turbulent viscosity expression exists for the curved flow in the channel cross-section nor a turbulence model can be applied for determining the turbulent viscosity unless the transverse bed velocity can be specified a priori.

Table 5: Transverse velocity equations comparison table

Description	Rozovskii (1961), Eq. (12)	Kikkawa *et al*. (1976), Eq. (13)	Ascanio and Kennedy (1983), Eq. (18)	Present approach, Eq. (39)
-Equation structure of form	Integral	Logarithmic	Infinite series	Ordinary power function
-Number of equations	3 equations: Eqs. (9-11)	3 equations: Eqs. (13-15)	Infinite	One
-Practicality to the hydraulic engineer	Less practical	Less practical	Extremely less practical	Practical
-Possibility of calculating lateral bed velocity	No	Yes	NA	Yes
-Inclusion of transverse surface forces (e.g. wind)	No	No	No	Yes
-Transverse Boundary shear stress	No	No	No	Yes
-Fully developed vertical profile	NA	NA	Yes	Yes

In summary, the accurate determination of turbulent viscosity for curved flow in the channel cross-section remains a challenge and no reliable expression or turbulence model exists for this purpose. The application of a turbulence model to determine turbulent viscosity is particularly challenging due to the requirement of specifying the transverse bed velocity in advance. However, obtaining the precise value of the transverse bed velocity is a complex task that currently lacks a robust solution. Therefore, the accurate estimation of turbulent viscosity in curved flow scenarios, as well as the application of turbulence models, is contingent upon the availability of a known transverse bed velocity, which remains a significant limitation in the field.

In conclusion, this study presents a novel contribution to the study of flow mechanics in meandering open channels. The developed equations for transverse velocity, transverse boundary shear stress, and deviation angles provide a comprehensive framework for understanding flow behavior in meandering channels. By incorporating previously neglected lateral forces such as wind forces, the proposed approach improves the accuracy and applicability of flow characterization. These findings have practical implications in hydraulics and river engineering and management, enabling better-informed decisions for the design and maintenance of meandering channels.

Conclusion

In conclusion, this study has significantly advanced our understanding of flow mechanics in curved meandering open channels by addressing gaps in previous methods and introducing novel equations. The developed equations consider important influencing variables, with a particular focus on channel roughness and lateral forces such as wind stress, and offer several advantageous properties. They are user-friendly, suitable for both analytical and numerical investigations, and represent a major improvement over the complex logarithmic, integral, or infinite series forms found in existing literature.

A key contribution of this study is the introduction of a new vertical distribution for transverse velocity using ordinary power functions. This simplicity allows for easier calculation of the transverse bed velocity and lateral boundary shear stress, overcoming the limitations associated with undefined logarithmic functions at the bed level. The developed equation for transverse velocity relies on two key assumptions. Firstly, it assumes a constant turbulent viscosity throughout the flow. Secondly, it relies on the condition that the topographic steering number is less than one, allowing for the approximation of mild curvature and meandering conditions. The proposed transverse velocity equation enables the calculation of the derivative of the velocity profile, providing an expression for the transverse boundary shear stress. Additionally, by substituting z = 0 directly into the equation, the transverse bed velocity can be obtained. The accuracy of the developed transverse velocity profile has been demonstrated through comparisons with established velocity profiles.

Importantly, the new velocity profile incorporates considerations for lateral wind shear stress and other lateral surface forces, which were not accounted for in previous velocity distributions. This inclusion provides a more comprehensive understanding of flow behavior in meandering channels and enhances the accuracy of predictions.

The analysis also highlights the significant impact of wind shear stress, with a wind stress of 0.5 Pa (corresponding to a speed of 10 m/s) resulting in a substantial 26% increase in transverse surface velocity and an 18% increase in transverse bed velocity. The expression for transverse boundary shear stress considers both the centripetal force and the transverse pressure force resulting from the transverse water surface slope. Furthermore, derived expressions for flow velocity deviation angle and bed shear stress deviation angle offer a clear distinction between the two angles, incorporating roughness, main velocity, water average depth, and channel radius of curvature.

The developed expression for lateral boundary shear stress can be effectively integrated into existing models to improve the calculation of transverse bed slope and lateral bed load rate. This advancement has the potential to enhance our understanding and prediction of sediment transport in curved meandering open channels.

Overall, the findings of this study and the developed equations significantly contribute to our knowledge of flow mechanics in curved meandering channels. They offer improved accuracy, usability, and the ability to account for essential variables that were previously overlooked. These advancements have important implications for river engineering and management, providing a more comprehensive framework for the design and maintenance of meandering channels.

Notation

The following symbols are used in this study:

$$F_1(\eta) = \int \frac{2\ln\eta}{\eta - 1}\, d\eta$$

$$F_2(\eta) = \int \frac{\ln^2\eta}{\eta - 1}\, d\eta$$

$$F_A(\eta) = -15\left[(\eta)^2\ln(\eta) - \frac{1}{2}(\eta)^2 + \frac{15}{54}\right]$$

$$F_B(\eta) = \frac{15}{2}\left[(\eta)^2\ln^2(\eta) - (\eta)^2\ln(\eta) + \frac{1}{2}(\eta)^2 - \frac{19}{54}\right]$$

$\bar{U}$ = The depth-averaged longitudinal velocity

v_b = The lateral bed velocity (at $z = 0$)
δ_v = An angle of deviation of the resultant velocity vector the channel tangential direction
δ_{vb} = The flow bed velocity deviation angle
δ_{vs} = The surface velocity deviation angle
$\delta_{\tau b}$ = The angle between the resultant bed shear stress and the channel axis
v_T = The isotropic turbulent eddy viscosity
τ_{or} = The radial component of the boundary shear stress
τ_{os} = The tangential boundary stress
τ_{rs} = The external radial surface shear stress acting on the water surface
B = The channel width
c = Constant taken as 0.0765
C = The Chezy's roughness coefficient
C_r = A correction factor that accounts for the nonlinear distribution of the main velocity
c_u = A coefficient depends on the flow conditions
D = The local flow depth
f = The Darcy-Welsbach friction factor
$F(r)$ = The radial distribution of the dimensionless depth-averaged main velocity
g = The acceleration due to gravity
k_s = A representative roughness height of the bed surface
m = An exponent in the primary-flow velocity power law = $\frac{1}{\kappa}\sqrt{\frac{f}{8}}$
n = Manning's roughness coefficient
p = Reciprocal of "m"
r = The radial direction measured from the center of curvature of the bend
r_c = The radius of the channel center line
S = The channel longitudinal slope
s = The curvilinear coordinate along the channel main direction
S_r = The transverse water surface slope
t = The time
U = The cross-sectional averaged-velocity
u = The primary (longitudinal or main) local flow velocity
u_* = The local shear velocity
U_* = The shear velocity of the cross-section
u_b = The bed's longitudinal or main velocity
v = the lateral (radial or transverse) local velocity
v_s = The value of the transverse velocity at the water surface
w = The vertical local velocity
z = The vertical coordinate measured from the bed level upward
z_b = The thickness or height of the longitudinal bed-load layer
η = Is the relative depth (= z/D)
κ = The von Karman constant
ρ = The fluid density
τ_r = The radial or transverse local turbulent-shear stress
τ_s = The longitudinal local turbulent shear stress
$\Phi(f) = \frac{(1+p)^2}{(2p+1)}$

Acknowledgment

The author would like to present his sincere gratitude and appreciation to anonymous reviewers for the very fruitful, informative and important remarks, suggestions and comments which really helped in significant improving of this manuscript.

Funding Information

This study has not received any funding.

Ethics

The author declares that he has no known competing financial interests or personal relationships that could have appeared to influence the work reported in this study and that this study adheres to the ethics.

References

Ascanio, M. F., & Kennedy, J. F. (1983). Flow in alluvial-river curves. *Journal of Fluid Mechanics*, *133*, 1–16. https://doi.org/10.1017/s0022112083001755

Bai, R., Zhu, D., Chen, H., & Li, D. (2019). Laboratory Study of Secondary Flow in an Open Channel Bend by Using PIV. *Water*, *11*(4), 659. https://doi.org/10.3390/w11040659

Benque, J. P., Cunge, J. A., Feuillet, J., Hauguel, A., & Holly, F. M. (1982). New Method for Tidal Current Computation. *Journal of the Waterway, Port, Coastal and Ocean Division*, *108*(3), 396–417. https://doi.org/10.1061/jwpcdx.0000311

Blanckaert, K. (2010). Topographic steering, flow recirculation, velocity redistribution, and bed topography in sharp meander bends. *Water Resources Research*, *46*(9). https://doi.org/10.1029/2009wr008303

Bridge, J. S. (1977). Flow, bed topography, grain size and sedimentary structure in open channel bends A three-dimensional model. *Earth Surface Processes*, *2*(4), 401–416. https://doi.org/10.1002/esp.3290020410

Chang, H. H. (1983). Energy Expenditure in Curved Open Channels. *Journal of Hydraulic Engineering*, *109*(7), 1012–1022. https://doi.org/10.1061/(asce)0733-9429(1983)109:7(1012)

Chang, H. H. (1984). Regular Meander Path Model. *Journal of Hydraulic Engineering*, *110*(10), 1398–1411. https://doi.org/10.1061/(asce)0733-9429(1984)110:10(1398)

Chang, H. H. (1988). *Fluvial processes in river engineering* (1st Ed.). John Wiley & Sons.

Dey, S., Mahato, R. K., & Ali, S. Z. (2023). Turbulent Shear Flow over a Downstream-Skewed Wavy Bed: Analytical Model Based on the RANS Equations with Boussinesq Approximation. *Journal of Hydraulic Engineering*, *149*(9), 04023028. https://doi.org/10.1061/jhend8.hyeng-13577

Dietrich, W. E., & Smith, J. D. (1983). Influence of the point bar on flow through curved channels. *Water Resources Research*, *19*(5), 1173–1192. https://doi.org/10.1029/wr019i005p01173

Elbagoury, D. H., Boegman, L., & Rao, Y. R. (2023). Modeling River Plume Dynamics in a Large Wind-Forced Embayment. *Journal of Hydraulic Engineering*, *149*(4), 05023001. https://doi.org/10.1061/jhend8.hyeng-13238

El-Ghorab, E. A. (1999). *Management of cooling systems of electrical power plants and its impact on the Nile River environment*. Institute of Environmental Studies and Research, Ain Shams University.

Engelund, F. (1974). Flow and Bed Topography in Channel Bends. *Journal of the Hydraulics Division*, *100*(11), 1631–1648. https://doi.org/10.1061/jyceaj.0004109

Ferreira da Silva, A. M., & Ebrahimi, M. (2017). Meandering Morphodynamics: Insights from Laboratory and Numerical Experiments and Beyond. *Journal of Hydraulic Engineering*, *143*(9), 03117005. https://doi.org/10.1061/(asce)hy.1943-7900.0001324

Fischer, H. B., List, E. J., Koh, R. C. Y., Imberger, J., & Brooks, N. H. (1979). Mixing in inland and coastal waters, Academic, New York, 104–138.

Gu, L., Zhang, S., He, L., Chen, D., Blanckaert, K., Ottevanger, W., & Zhang, Y. (2016). Modeling Flow Pattern and Evolution of Meandering Channels with a Nonlinear Model. *Water*, *8*(10), 418. https://doi.org/10.3390/w8100418

Hafez Y. I. (1995). A k-ε Turbulence Model for Predicting the Three-Dimensional Velocity Field and Boundary Shear in Open and Closed Channels. Ph.D. Dissertation, Civil Engineering Department, Colorado State University, Fort Collins, Colorado, USA, https://mountainscholar.org/handle/10217/235417

Hafez, Y. I. (2022). Excess energy theory for river curvature and meandering. *Journal of Hydrology*, *608*, 127604. https://doi.org/10.1016/j.jhydrol.2022.127604

Hafez, Y. I. (2023). Transverse energy loss slope in meandering channels. *Journal of Hydro-Environment Research*, *51*, 1–14. https://doi.org/10.1016/j.jher.2023.08.002

He, L. (2018). Distribution of primary and secondary currents in sine-generated bends. *Water SA*, *44*(1), 118–129. https://doi.org/10.4314/wsa.v44i1.14

He, L., Chen, D., Termini, D., Zhang, S., & Zhu, Z. (2021). Experiments on Longitudinal and Transverse Bedload Transport in Sine-Generated Meandering Channels. *Applied Sciences*, *11*(14), 6560. https://doi.org/10.3390/app11146560

Jansen, P. P., Bendegom, L., Berg, J., Vries, M., & Zanen, A. (1979). *Principals of river engineering*. Pitman.

Kheireldin, K. (1995). *Shear stress and stream power distribution around vertical wall abutments*. Civil Engineering Department, Colorado State University, Fort Collins.

Kikkawa, H., Kitagawa, A., & Ikeda, S. (1976). Flow and Bed Topography in Curved Open Channels. *Journal of the Hydraulics Division*, *102*(9), 1327–1342. https://doi.org/10.1061/jyceaj.0004615

Kimura, I., & Hosoda, T. (1997). Fundamental Properties of Flows in Open Channels with Dead Zone. *Journal of Hydraulic Engineering*, *123*(2), 98–107. https://doi.org/10.1061/(asce)0733-9429(1997)123:2(98)

Krzyk, M., & Cetina, M. (2018). Analysis of flow in a curved channel using the curvilinear orthogonal numerical mesh. *Journal of Mechanical Engineering*, *64*(9), 536. https://doi.org/10.5545/sv-jme.2017.5183

Kondrat′ev, N. E. (1959). *River flow and river channel formation*. Israel program.

Laufer, J. (1951). *Investigation of turbulent fow in a two-dimensional channel*. NACA.

Li, B., Xu, H., Bai, Y., & Ji, Z. (2022). Hydrodynamic Structure and Turbulent Characteristics of Low-Slope Bedrock Bend Reach with Constant Curvature. *Journal of Hydraulic Engineering*, *148*(9), 06022009. https://doi.org/10.1061/(asce)hy.1943-7900.0001995

Makhail, R., Chu, V. H., & Savaoe, S. B. (1975). The reattachment of a two dimensional turbulent jet in a confined cross flow. *Proceedings of the 16th IAHR Congress*, 414–419.

Molinas, A., & Hafez, Y. I. (2000). Finite element surface model for flow around vertical wall abutments. *Journal of Fluids and Structures*, *14*(5), 711–733. https://doi.org/10.1006/jfls.2000.0295

Nowroozpour, A., Ettema, R., & Fakhri, A. (2022). A Reassessment of Contraction Scour at Bridge Waterways. *Journal of Hydraulic Engineering*, *148*(12), 06022016. https://doi.org/10.1061/(asce)hy.1943-7900.0002031

Odgaard, A. J. (1981). Transverse Bed Slope in Alluvial Channel Bends. *Journal of the Hydraulics Division*, *107*(12), 1677–1694. https://doi.org/10.1061/jyceaj.0005784

Odgaard, A. J. (1982). Bed Characteristics in Alluvial Channel Bends. *Journal of the Hydraulics Division*, *108*(11), 1268–1281. https://doi.org/10.1061/jyceaj.0005932

Odgaard, A. J. (1984). Grain-Size Distribution of River-Bed Armor Layers. *Journal of Hydraulic Engineering*, *110*(10), 1479–1484. https://doi.org/10.1061/(asce)0733-9429(1984)110:10(1479)

Odgaard, A. J. (1986a). Meander Flow Model. I: Development. *Journal of Hydraulic Engineering*, *112*(12), 1117–1135. https://doi.org/10.1061/(asce)0733-9429(1986)112:12(1117)

Odgaard, A. J. (1986b). Meander Flow Model. II: Applications. *Journal of Hydraulic Engineering*, *112*(12), 1137–1149. https://doi.org/10.1061/(asce)0733-9429(1986)112:12(1137)

Park, S. W., & Ahn, J. (2019). Experimental and numerical investigations of primary flow patterns and mixing in laboratory meandering channel. *Smart Water*, *4*(1), 1–15. https://doi.org/10.1186/s40713-019-0016-y

Parker, G. (1984). Discussion of "Lateral Bed Load Transport on Side Slopes" by Syunsuke Ikeda (November, 1982). *Journal of Hydraulic Engineering*, *110*(2), 197–199. https://doi.org/10.1061/(asce)0733-9429(1984)110:2(197)

Pradhan, A., Kumar Khatua, K., & Sankalp, S. (2018). Variation of Velocity Distribution in Rough Meandering Channels. *Advances in Civil Engineering*, *2018*, 1–12. https://doi.org/10.1155/2018/1569271

Rajaratnam, N., & Nwachukwu, B. A. (1983). Flow Near Groin-Like Structures. *Journal of Hydraulic Engineering*, *109*(3), 463–480. https://doi.org/10.1061/(asce)0733-9429(1983)109:3(463)

Rastogi, A. K., & Rodi, W. (1978). Predictions of Heat and Mass Transfer in Open Channels. *Journal of the Hydraulics Division*, *104*(3), 397–420. https://doi.org/10.1061/jyceaj.0004962

Roberson, J. A., & Crowe, C. T. (1985). *Engineering Fluid Mechanics* (3rd ed.). Houghton Mifflin Company.

Rodi, W. (2000). Turbulence Models and Their Application in Hydraulics (1st Ed.). Routledge. https://doi.org/10.1201/9780203734896

Rozovskii, I. L. (1961). *Flow of Water in Bends of Open Channels*. Academy of Sciences of the Ukrainian SSR.

Sahagian, D., Diplas, P., Urban, C., Cheng, Z., & David, M. (2022). In search of a unifying criterion for meandering systems: examples from natural and built environments. *Environmental Fluid Mechanics*, *22*(2), 467–494. https://doi.org/10.1007/s10652-022-09851-8

Strazisar, A., & Prahl, J. (1973). The effects of bottom friction on river entrance flow with crossflow. *Proceedings of the 16th Conference on Great Lakes Research*, 615–625.

Talaa, A. M., Y.I., H., Rashad, R. M., & Abdallh, E. (2002). Prediction of Heat and Mass Transfer Affecting Open Channels Environment. *Journal of Environmental Science, Ain Shams University*, *4*(3).

Tan, W. (1992). *Shallow water Hydrodynamics* (Vol. 55). Water & Power Press.

Thangam, S., & Speziale, C. G. (1992). Turbulent flow past a backward-facing step - A critical evaluation of two-equation models. *AIAA Journal*, *30*(5), 1314–1320. https://doi.org/10.2514/3.11066

Thappeta, S. K., Bhallamudi, S. M., Chandra, V., Fiener, P., & Baki, A. B. M. (2020). Energy Loss in Steep Open Channels with Step-Pools. *Water*, *13*(1), 72. https://doi.org/10.3390/w13010072

Weiss, S. F., & Higdon, J. J. L. (2022). Dynamics of meandering rivers in finite-length channels: linear theory. *Journal of Fluid Mechanics*, *938*, A11. https://doi.org/10.1017/jfm.2022.131

Yen, B. C. (1965). *Characteristics of subcritical flow in a meandering channel*. Institute of Hydraulic Research.

Zhou, T., & Endreny, T. (2020). The Straightening of a River Meander Leads to Extensive Losses in Flow Complexity and Ecosystem Services. *Water*, *12*(6), 1680. https://doi.org/10.3390/w12061680

Zhou, Y., & Tang, Q. (2022). Meandering Characteristics of the Yimin River in Hulun Buir Grassland, Inner Mongolia, China. *Remote Sensing*, *14*(11), 2696. https://doi.org/10.3390/rs14112696

Zimmerman, C., & Kennedy, J. F. (1978). Transverse Bed Slopes in Curved Alluvial Streams. *Journal of the Hydraulics Division*, *104*(1), 33–48. https://doi.org/10.1061/jyceaj.0004922